BACTERIAL CELLULOSE PRODUCTION FROM OIL PALM FROND JUICE AND ITS IMPREGNATION WITH SILVER NANOPARTICLES FOR ANTIBACTERIAL WOUND DRESSING

TAN SOU MIN[1]; NOR SYAHIRAH ABD KARIM[1]; SHAHRIL MOHAMAD[1]; JUNAIDI ZAKARIA[1]; MOHD HAFIZ ARZMI[2]; HASSAN FAHMI ISMAIL[3] and ROHANA ABU[1]*

ABSTRACT

Bacterial cellulose-silver nanoparticles (BC-AgNPs) composite was prepared for a bacterial wound dressing. The oil palm frond (OPF) juice was utilised as a low-cost raw material for BC production. The AgNPs were incorporated in the BC composite by thermal reduction of 1 mM silver nitrate for their antibacterial agent. The BC-AgNPs composite had dense nanofibrils with an average diameter of 61.5 ± 1.0 nm as shown in the field emission scanning electron microscope (FESEM) images. The composite had a crystallinity index of 86.5% and the nanoparticles had a face-centred cubic geometry with a crystal size of 26.5 nm as determined by X-ray diffraction analysis (XRD). The Ag content was 1.463 mg/100 cm^2 in the composite analysed by atomic absorption spectrophotometry (AAS). 10.4% of the total Ag content was released from AgNPs in 72 hr as measured by inductively coupled plasma mass spectrometry (ICP-MS). The composite also demonstrated excellent antibacterial action against Staphylococcus aureus, giving a 29 ± 0.8 mm inhibition zone by the disk diffusion assay. Pure BC composite exhibited no cytotoxicity effect on the HSF1184 fibroblast cells and 10%-40% BC-AgNPs composite extracts were compatible with the cell growth. The study suggests the BC-AgNPs composite is a good material for antibacterial wound dressing.

INTRODUCTION

The developments of new value-added products from agricultural biomass as low-cost raw materials are of great prospects in various fields such as biocompost, biofuel, bioplastic and biomaterial (Aziz *et al.*, 2023; Harrison *et al.*, 2023). Most palm oil-producing countries like Malaysia and Indonesia contribute significant biomass resources including oil palm trunk (OPT) and oil palm frond (OPF). The OPF is generated after fruit harvesting at the plantation area and it was estimated that 42 million tonnes/yr of OPF were abundantly available (Gan *et al.*, 2023). Various value-added products have been developed due to the availability of biomass resources from the sustainable Malaysian palm oil industry (Parveez *et al.*, 2023; Rashidi *et al.*, 2022). The current industrial utilisation of OPF is in producing paper, animal feed, bio-alcohol, bio-char and biogas (Gan *et al.*, 2023; Norrrahim *et al.*, 2022; Zakaria *et al.*, 2023). More recently, the OPF juice which contains high-carbon sugars has been found suitable to be utilised as a low-cost fermentation medium for bacterial growth in bacterial cellulose production (BC) (Lim *et al.*, 2022; Mohamad *et al.*, 2022; Said Azmi *et al.*, 2023).

1   Faculty of Chemical and Process Engineering Technology, Universiti Malaysia Pahang Al-Sultan Abdullah, 26300 Kuantan, Pahang, Malaysia.

2   Department of Fundamental Dental and Medical Sciences, Kulliyyah of Dentistry, International Islamic University Malaysia, 25200 Kuantan, Pahang, Malaysia.

3   Institute of Marine Biotechnology, Universiti Malaysia Terengganu, 21030 Kuala Terengganu, Terengganu, Malaysia.

*   Corresponding author e-mail: rohanaa@umpsa.edu.my

BC composite is an extracellular product mainly synthesised by *Komagataeibacter xylinus*, a cellulose-producing bacteria also known as *Acetobacter xylinus* and *Gluconacetobacter xylinus*. This product is considered suitable for treating wounds because of its high purity and crystallinity with good mechanical strength, water holding capacity and biocompatibility (Avcioglu, 2022). The application of BC composite as a wound dressing has been reported to promote cell adhesion, proliferation and differentiation in wound healing phases, including hemostasis, inflammation, proliferation, and remodelling (Pang *et al.*, 2020).

Despite its excellent role as a wound dressing, bacterial infection is still a concern as BC does not have intrinsic antibacterial properties that limit its application. BC-based antibacterial wound dressing can be developed by incorporating antibacterial agents into the BC matrix to prevent possible bacterial infection (Alyamani *et al.*, 2023). BC's nanofibril network has been found to facilitate the penetration of various antibacterial agents through different impregnation methods that attracted many researchers' attention recently (Chandana *et al.*, 2022). Interestingly, the BC containing inorganic nanoparticles like Ag, Au, CuO and ZnO showed significant efficacy against bacterial pathogens like *Staphylococcus aureus*, *Candida albicans*, *Escherichia coli*, *Salmonella enterica* and *Pseudomonas aeruginosa* (Araújo *et al.*, 2018; Ayyappan *et al.*, 2022; Heidari *et al.*, 2022; Shaaban *et al.*, 2023). Skin cells such as keratinocytes and fibroblasts have also demonstrated good biocompatibility with the BC composite loaded with nanoparticles (Sabarees *et al.*, 2022). Moreover, our recent study has shown that AgNPs impregnated into BC composite can provide a favourable moisture environment with good water holding and release properties comparable to pure BC (Abu *et al.*, 2021; 2022).

Therefore, this study aimed to develop the BC-AgNPs composite for bacterial wound dressing. The BC was produced using the OPF juice by *A. xylinum* and subsequently, the BC was impregnated with AgNPs by hydrothermal reduction. The composite properties were further analysed by FTIR, FESEM and XRD. The Ag content in the composite and the slow release of Ag$^+$ ions from the composite were measured by AAS and ICP-MS, respectively. The antibacterial activity against *S. aureus* was studied using the disk diffusion assay and the biocompatibility was tested in human skin fibroblast HSF1184 cells using the MTT assay.

MATERIALS AND METHODS

Materials

Silver nitrate was purchased from Bendosen Laboratory Chemicals, Norway. Acetic acid, sulphuric acid, nitric acid and MTT [3-(4,5-dimethylthiazol-2-yl)-2,5-diphenyltetrazolium bromide] were acquired from Sigma-Aldrich, USA. Sodium hydroxide was procured from R&M Chemicals, UK. Bacterial strain *A. xylinum* 0416 was bought from MARDI (Malaysian Agriculture and Research Development Institute). *Staphylococcus aureus* ATCC 6538 and human skin fibroblasts HSF1184 were provided by IIUM (International Islamic University Malaysia) and UMT (University Malaysia Terengganu), respectively.

Production of BC by OPF Juice

OPF petioles were collected at LCSB Lepar palm oil plantation, Pahang. The petioles were mechanically pressed to extract the OPF juice. Before being autoclaved at 121°C for 10 min, the pH of the fermentation medium (60% v/v) was adjusted to 4.0 using 50% v/v acetic acid. 10% v/v *A. xylinum* 0416 inoculum was cultivated in 24-well plates and statically incubated at 30°C for 10 days (Mohamad *et al.*, 2022). The boiling NaOH solution was used to purify the BC composites for 20 min. The composites were then stored at 4°C after soaking in distilled water.

BC-AgNPs by Hydrothermal Reduction

BC composite was submerged in a glass vial containing 25 mL of 1.0 mM AgNO$_3$ solution. The vial was wrapped with aluminium foil and autoclaved for 10 min at 121°C and 0.103 MPa for hydrothermal reduction. The composite was left at room temperature in distilled water to stop the reduction process. After that, it was freeze-dried for 24 hr at -70°C and 0.011 Mba before the characterisation studies.

BC-AgNPs Characterisation

The cellulose functional groups present in the BC-AgNPs composite were identified using Fourier transform infrared (FTIR) spectroscopy (Thermo-Scientific NICOLET iS50), equipped with the attenuated total reflectance (ATR). The average of each spectrum was 16 scans in the range of 4000 to 500 cm^{-1} at 4 cm^{-1} spatial resolution. The surface morphology of sputter-coated platinum of BC and BC-AgNPs composites was identified at 5 kV acceleration voltage using a JEOL JSM-7800F field emission-scanning electron microscope (FESEM). The size distribution was analysed by histogram using ImageJ software. The presence of elemental silver in the composite was determined by Energy dispersive X-ray (EDX) attached to the FESEM. The crystalline structure of the composite was analysed by a PANalytical X'Pert Pro X-ray diffractometer (XRD) using Cu Kα irradiation at λ =1.54060A°. The XRD data was measured in 2θ between 10°-80° range at 1° per min scan speed. The crystallite index and

size were calculated using empirical method (Zeng *et al.,* 2014) and Scherrer equation (Manosalva *et al.,* 2019), respectively.

Silver Content and Release Studies

The quantity of silver in the BC-AgNPs composite was measured by flame atomic absorption spectrometry (AAS) (Hitachi Z-5000 Polarized Zeeman, Japan). The composite was heated for 2 hr at 600°C using a furnace. The remaining substance was dissolved in 2 mL of concentrated nitric acid before diluting to 100 mL with distilled water for AAS analysis. The Ag^+ ions released from the composite were measured using inductively coupled plasma mass spectrometry analysis (ICP-MS) (7500a Agilent Technologies, USA). The composite was immersed in 10 mL of PBS solution at pH 7.4 and was placed in a water bath at 37°C. 200 μL of the solution was taken at 1.5, 2.5, 6, 24, 48 and 72 hr for the analysis.

Antibacterial Activity

The antibacterial susceptibility testing was conducted using the disk diffusion method. The inhibitory effect of AgNPs in the BC composite was assessed on the bacterial strain *S. aureus* grown onto the Mueller Hinton agar plate after overnight incubation at 37°C. The diameter of zone inhibition was measured in three biological replicates.

Cytotoxicity Test

The *in vitro* cytotoxicity test was conducted using Human skin fibroblast HSF1184 cells. Cell culture medium was prepared using Dulbecco's Modified Eagle's Medium (DMEM) supplemented with 10% fetal bovine serum and 1% penicillin-streptomycin (Invitrogen, CA, USA). 1.0×10^4 cells per well were cultured in 96-well plates and incubated overnight at 37°C, 5% CO_2, and 95% humidity. After removing the medium, the cells were treated with BC composite extract and the serially diluted BC-AgNPs extract in DMEM (100%, 80%, 60%, 40% and 10%) for 24 hr (Horue *et al.,* 2020). Cells that were treated with only DMEM were used as a control. After the treatment, 100 μL MTT solution was added to each well and then incubated for an additional 3 hr. The formed MTT formazan was dissolved with 100 mL of dimethyl sulfoxide and the solution's absorbance was measured at 570 nm using an ELISA microplate reader.

Statistical Analysis

Statistical analysis was performed using Origin 2022 software (OriginLab, Northampton, MA, USA). Results are expressed as mean value ± standard error of the mean. The statistical significance of the results was determined using Student's T-test ($P \leq 0.05$).

RESULTS AND DISCUSSION

Synthesis of BC-AgNPs Composite

Prior studies found that the pressed juice from OPF has a high concentration of fermentable sugar, which can be utilised as a cheap carbon source for microbial growth in BC production (Mohamad *et al.,* 2022; Said Azmi *et al.,* 2023). The BC yield can be obtained up to 2.33 g/L using 60% v/v of OPF juice after 14 days of static fermentation (Mohamad *et al.,* 2022). In this study, the BC was produced using the same fermentation conditions with a shorter incubation time of 10 days as a thick BC film was obtained due to a lower surface area of 24-well plates. The produced BC was then hydrothermally incorporated with AgNPs to explore its potential use as an antibacterial wound dressing. It was found that the pure BC composite was colourless while the BC-AgNPs composite was yellowish, indicating that AgNPs were successfully incorporated into the BC composite. The schematic representation in *Figure 1* served as an illustration of how the BC-AgNPs composite was developed.

Characterisation of BC-AgNPs Composite

From the FESEM images, the nanofibril mean diameter of 60.2 ± 1.5 nm was obtained with the loose arrangement in the pure BC composite (*Figure 2a*). While the BC-AgNPs composite exhibits denser cellulose fibrils with a mean diameter of 61.5 ± 1.0 nm and the presence of 24.7 ± 2.9 nm mean diameter of Ag spherical particle attached to the surface of nanofibrils (*Figure 2b* and *2c*). It can be seen from the image that each particle is either individually or aggregately attached to the nanofibril surface. The presence of elemental Ag on the surface was also confirmed by the EDX analysis as shown in the EDX spectrum (*Figure 2d*). A similar characteristic was also observed in other BC-AgNPs studies (Pal *et al.,* 2017; Shidlovskiy *et al.,* 2018).

BC produced from OPF juice shows the typical FTIR spectra of cellulose with broad vibration at 3335 cm^{-1} and 1625 cm^{-1}, indicating the OH stretching of the hydroxyl group (Pal *et al.,* 2017) and the C=O stretching of the carbonyl group (Liu *et al.,* 2015), respectively. These functional groups exhibit good hydrophilicity for the BC composite. Similarly, the BC-AgNPs composite had the same strong peaks but a shift occurred in the spectra (*Figure 3*). The same spectra suggest that the cellulose structure was maintained after the impregnation of AgNPs.
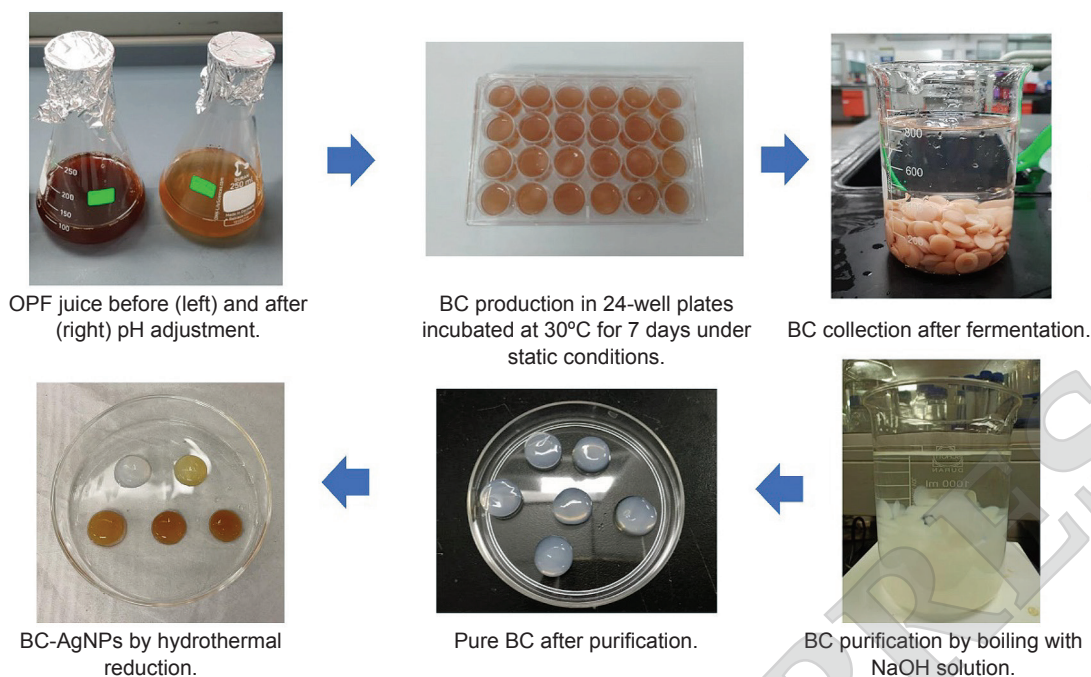
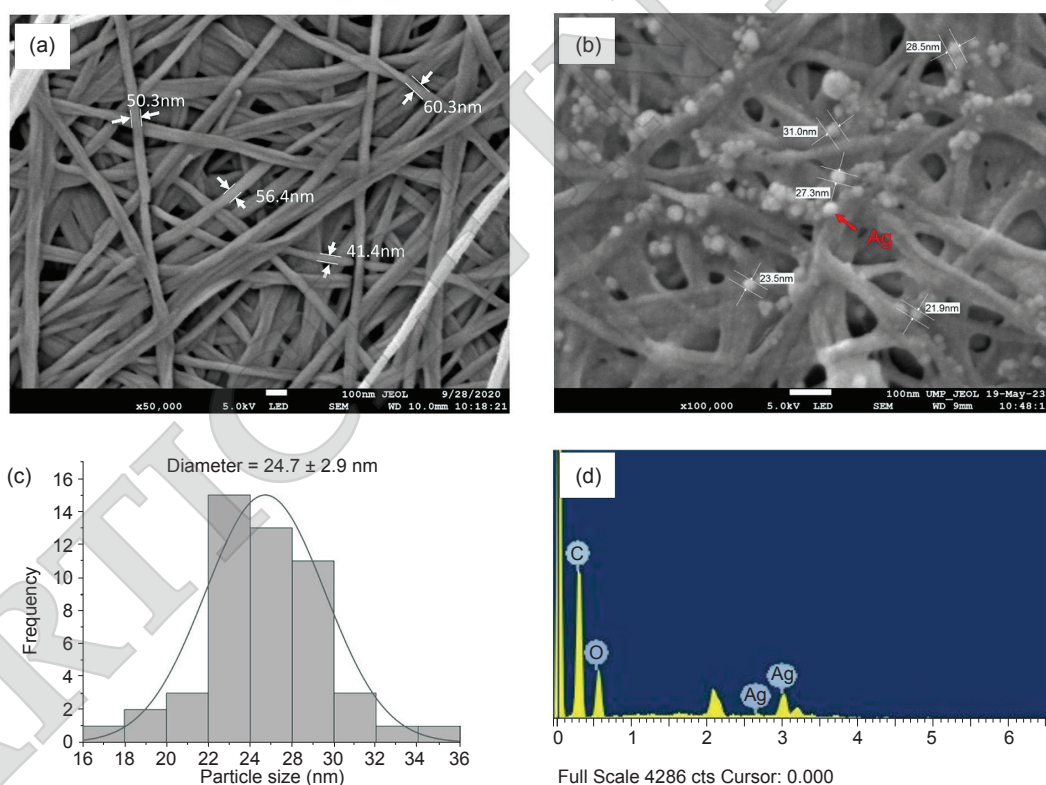*Figure 1. Schematic diagram of the development of the BC-AgNPs composite.*

OPF juice before (left) and after (right) pH adjustment.

BC production in 24-well plates incubated at 30ºC for 7 days under static conditions.

BC collection after fermentation.

BC-AgNPs by hydrothermal reduction.

Pure BC after purification.

BC purification by boiling with NaOH solution.

Figure 2. FESEM images of (a) pure BC, (b) BC-AgNPs, (c) particle size distribution of BC-AgNPs, and (d) EDX spectrum of BC-AgNPs. The red arrow indicates the elemental Ag.

XRD was used to identify the possible structural change in the BC-AgNPs composite compared to pure BC (*Figure 4*). The XRD pattern of pure BC had three typical diffraction peaks of crystalline cellulose I at 14.4°, 16.7° and 22.6° which correspond to the crystal planes of (1$\bar{1}$0), (110), and (200), respectively (Li *et al.*,

2015). BC-AgNPs composite had the same crystalline structure of cellulose I with the additional crystalline peaks of face-centred cubic (FCC) of AgNPs (Ganesh Babu and Gunasekaran, 2009). The FCC peaks can be seen at 38.2°, 44.1°, 64.4° and 77.4° which correspond to the crystal planes of (111), (200), (220) and (311),
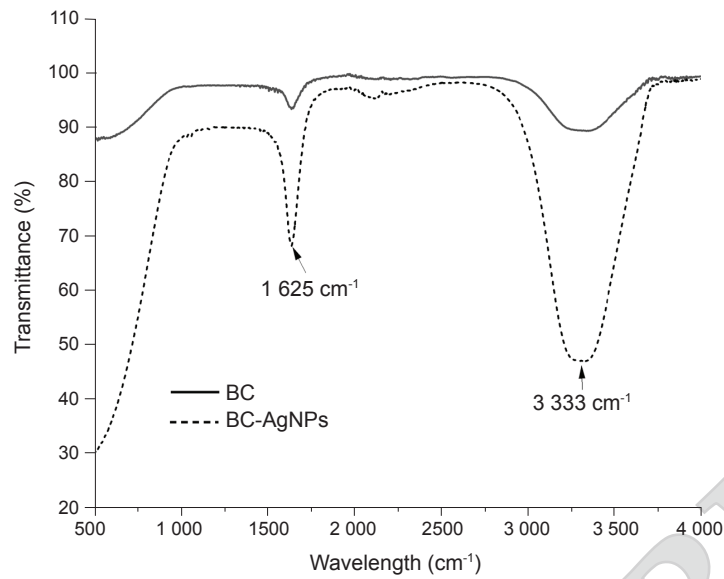
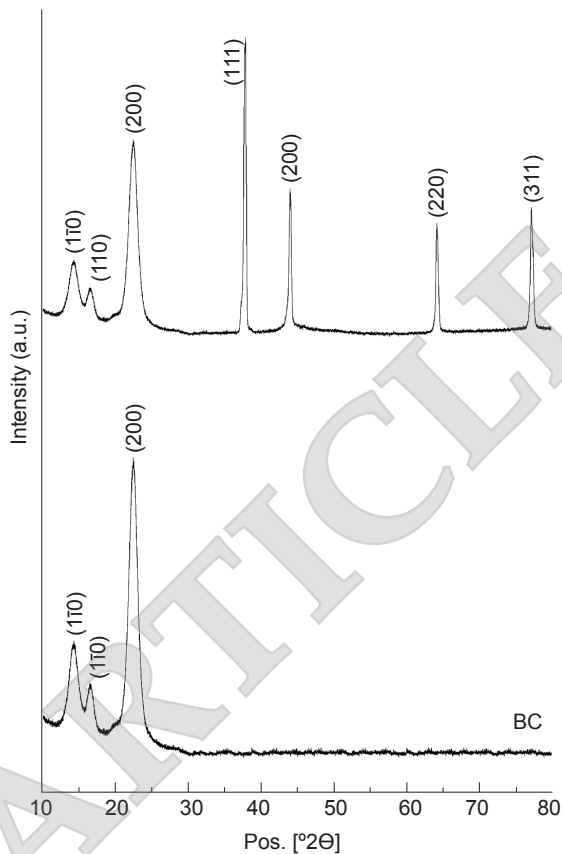*Figure 3. FTIR spectra of BC and BC-AgNPs.*

Figure 4. XRD patterns of BC and BC-AgNPs composites.

respectively. The crystallinity index of the BC-AgNPs composite had slightly decreased to 86.5% from 87.0% of the BC composite, showing minor structural change from the hydrothermal method. Moreover, the Ag in the BC composite had a nanosized crystal of 26.5 nm, calculated using the Scherrer equation.

Silver Content and Release of BC-AgNPs Composite

The Ag content in the BC-AgNPs composite was determined by AAS analysis. It was found that 1.463 mg of Ag was incorporated into 100 cm^2 of BC-AgNPs composite when prepared using 1 mM AgNO$_3$ concentration. The result is comparable to those reported in previous studies with values ranging from 0.04-16.00 mg Ag per 100 cm^2 composite, using the same hydrothermal method to prepare BC-AgNPs composite (Li *et al.*, 2015; Volova *et al.*, 2018).

The Ag ions profile diffused from the BC-AgNPs composite into the PBS solution at pH 7.4 and 37°C was demonstrated in *Figure 5*. It can be seen that the Ag$^+$ ions released rapidly in the initial 6 hr. After that, the release rate was sustained slowly until it reached a plateau. There was 10.4% of the total Ag$^+$ ions deposited from the composite in 72 hr. The initial rapid release of Ag$^+$ ions into PBS solution can be due to the fast ionisation of AgNPs that adhered on the nanofibril surface as shown in FESEM image. Besides, the slow-release rate of Ag$^+$ ions from the composite may be elucidated by the strong electrostatic interaction between the Ag$^+$ ions and the hydroxyl group of cellulose. The free ions are associated with the antibacterial potential of this composite. Excessive release of antibacterial agents can harm human cells and limit their antibacterial efficacy (Pal *et al.*, 2017).

Antibacterial Activity of BC-AgNPs Composite

The susceptibility of *S. aureus* ATCC 6538 towards antibacterial agent in BC composite was observed using the disk diffusion method.
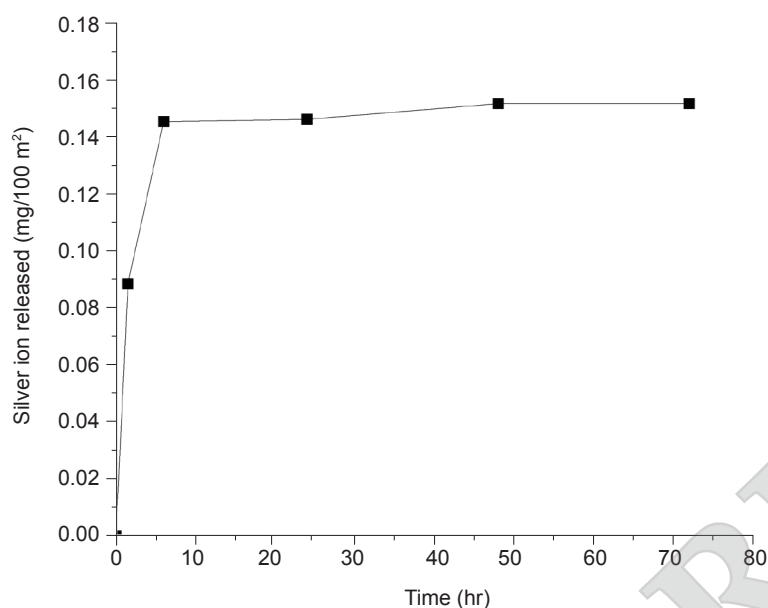
Figure 5. Ions released from BC-AgNPs composite as a function of the incubation time in PBS solution at 37°C and pH 7.4. The value was measured using inductively coupled plasma mass spectrometry (ICP-MS) analysis.

As expected, there was no inhibition for the BC composite indicating that the composite itself did not have antibacterial property against the bacterial strain which limits its wound dressing application (*Figure 6a*). Remarkably, the large inhibition zone of 29 ± 0.8 mm was measured for the BC-AgNPs composite, showing the susceptibility of *S. aureus* to the bactericidal effect of AgNPs (*Figure 6b*). Likewise, the effect was observed in other studies where the inhibition zones of 15 mm (Volova *et al*., 2018) and 9 mm (Yang *et al*., 2012) were shown by BC-AgNPs composites prepared by 1 mM AgNO$_3$ against the Gram-positive bacterium *S. aureus*. The different inhibition zone values may be caused by the use of different impregnation methods as well as the quantity of Ag$^+$ ions released from the BC composites (Wu *et al*., 2014).

Besides, the different biological activity of AgNPs can also be affected by several factors including particle size, morphology, surface charge, surface chemistry, capping agents as well as microorganism type (Barabadi *et al*., 2020; Saravanan *et al*., 2021; Talank *et al*., 2022). The high susceptibility of gram-positive bacteria to BC-AgNPs composite might be due to the strong electrostatic force between Ag ions that are released from the AgNPs and the sulphur proteins on the bacterial cell wall and cytoplasm membrane. The accumulation of the ions on the cell wall and cytoplasm membrane eventually causes cell disruption (More *et al*., 2023). AgNPs might also induce reactive oxygen species (ROS) formation in the cell which leads to the damage of DNA and membrane proteins (Talank *et al.,* 2022).

In addition to their excellent antibacterial activity, AgNPs have other biological potential such as antiviral (Barabadi *et al*., 2022a), antiparasitic (Jain *et al*., 2021), biofilm inhibitory (Barabadi *et al*., 2022b; Ibraheem *et al*., 2022), and antioxidant (Alzubaidi *et al*., 2023; Barabadi *et al*., 2020). The combination of BC with these biological activities is a feasible research direction for wound treatment.

Cytotoxicity of BC-AgNPs Composite

For wound healing applications, the dressing material must be biocompatible with skin cells. The cytotoxicity of BC-AgNPs composite was evaluated in human skin fibroblast HSF1184 cells using MTT assay. After 24 hr of exposure, the BC composite extract was found to be non-toxic to the cell lines when compared to control cells (*Figure 7*). The results are in agreement with previously reported biocompatibility of BC composite produced from various carbon sources (Jutakridsada *et al*., 2023; Lin *et al*., 2013; Qiu *et al*., 2016; Wu *et al*., 2014). Besides, the BC-AgNPs composite extracts showed non-toxicity up to 40% dilution after 24 hr of incubation. Nevertheless, 60% and 80% BC-AgNPs extracts started to inhibit fibroblast growth. This is because the antibacterial agent like AgNPs cannot differentiate between healthy cells and pathogenic bacteria. To some extent, the cytotoxic effects on cell growth strongly correlate with the amount of Ag in the composite and the amount of Ag$^+$ ions released from the composite (Jabbari and Babaeipour, 2023). Therefore, *in vitro* study is needed to test the biocompatibility of potential dressing material.
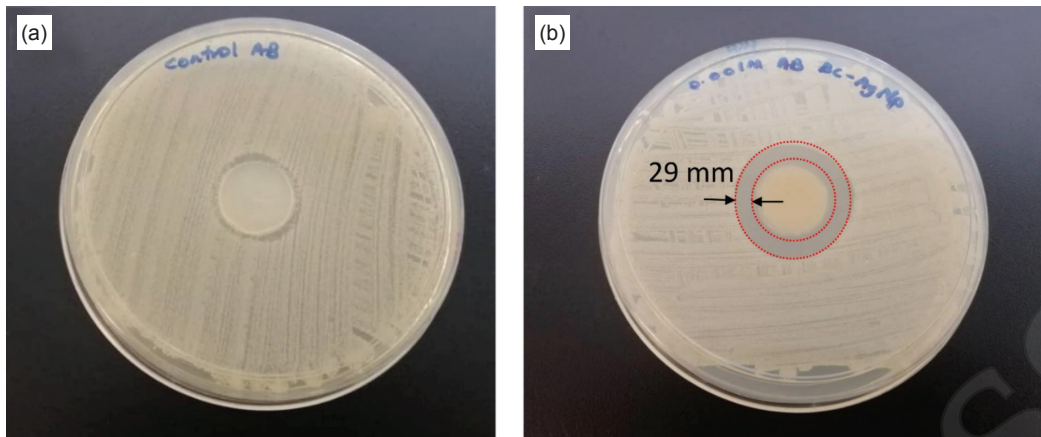
Figure 6. Antibacterial activity against Staphylococcus aureus *by the disk diffusion method. (a) No inhibition zone of
BC composite and (b) inhibition zone of 29 ± 0.8 mm of BC-AgNPs composite.*
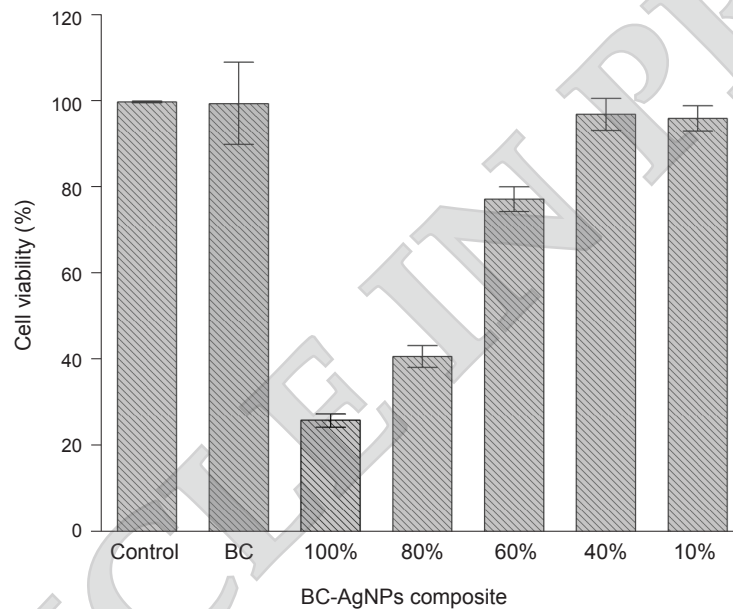

*Figure 7. Cytotoxicity of BC-AgNPs composite after 24 hr incubation in HSF1184 cell lines using MTT assay. In the
figure, control (untreated cells), BC composite and BC-AgNPs composite extracts in serial dilutions (10% to 100%). The
results were expressed in the mean ± standard error (n = 3).*

CONCLUSION

In summary, we prepared BC composite from OPF
juice and incorporated AgNPs into the composite
through hydrothermal synthesis. The results from
characterisation studies confirmed the incorporation
of AgNPs in the BC matrix was successful with
the presence of 24.7 ± 2.9 nm mean diameter of
Ag spherical particle attached to the surface of BC
nanofibrils. The slow release of Ag^+ ions from the
composite as analysed by ICP-MS might prevent
wound infection. The composite exhibits excellent
antibacterial activity with inhibition zone of 29 ± 0.8
mm against a gram-positive bacterium *S. aureus* and
good biocompatibility in fibroblast cell growth. This
study showed oil palm biomass could be efficiently
used for BC production and the developed BC-
AgNPs composite has the potential as a bacterial
wound dressing. Future research is necessary to
determine the biological potential of the BC-AgNPs
composite for ideal wound dressing.

REFERENCES

Abu, R; Mohamad, S; Zakaria, J; Mortan, S H and Yah, N A (2021). Water holding capacity and water release rate of bacterial cellulose-silver nanoparticles. *Proc. of Malaysian Technical Universities Conference on Engineering and Technology.* p. 472-473.

Abu, R; Mohamad, S; Zakaria, J; Mohd Amin, W N and Yin, C G C (2022). Water holding and release properties of bacterial cellulose produced from oil palm frond juice. *Mater. Sci. Forum, 1056*: 179-184.

Alyamani, A A; Al-Musawi, M H; Albukhaty, S; Sulaiman, G M; Ibrahim, K M; Ahmed, E M; Jabir, M S; Al-karagoly, H; Aljahmany, A A and Mohammed, M K A (2023). Electrospun polycaprolactone/chitosan nanofibers containing *Cordia myxa* fruit extract as potential biocompatible antibacterial wound dressings. *Molecules*, 28: 2501.

Alzubaidi, A K; Al-Kaabi, W J; Ali, A A; Albukhaty, S; Al-Karagoly, H; Sulaiman, G M, Asiri, M and Khane, Y (2023). Green synthesis and characterization of silver nanoparticles using flaxseed extract and evaluation of their antibacterial and antioxidant activities. *Appl. Sci.*, 13: 2182.

Araújo, I M S; Silva R R; Pacheco, G; Lustri, W R; Tercjak, A; Gutierrez, J; Júnior, J R S; Azevedo, F H C; Figuêredo, G S; Vega, M L; Ribeiro, S J L and Barud, H S (2018). Hydrothermal synthesis of bacterial cellulose–copper oxide nanocomposites and evaluation of their antimicrobial activity. *Carbohydr. Polym.*, 179: 341-349.

Avcioglu, N H (2022). Bacterial cellulose: Recent progress in production and industrial applications. *World J. Microbiol. Biotechnol.*, *38(5)*: 1-13.

Ayyappan, V G; Vhatkar, S S; Bose, S; Sampath, S; Das, S K; Samanta, D and Mandal, A B (2022). Incorporations of gold, silver and carbon nanomaterials to kombucha-derived bacterial cellulose: Development of antibacterial leather-like materials. *J. Indian Chem. Soc.*, *99(1)*: 100278.

Aziz, T; Haq, F; Farid, A; Kiran, M; Faisal, S; Ullah, A; Ullah, N; Bokhari, A; Mubashir, M; Chuah, L F and Show, P L (2023). Challenges associated with cellulose composite material: Facet engineering and prospective. *Environ. Res.*, 223: 115429.

Barabadi, H; Jounaki, K; Pishgahzadeh, E; Morad, H; Sadeghian-Abadi, S; Vahidi, H and Hussain, C M (2022a). Antiviral potential of green-synthesized silver nanoparticles. *Handbook of Microbial Nanotechnology* (Chaudery, M H ed.). Elsevier. p. 285-310.

Barabadi, H; Mohammadzadeh, A; Vahidi, H; Rashedi, M; Saravanan, M; Talank, N and Alizadeh, A (2022b). *Penicillium chrysogenum* derived silver nanoparticles: exploration of their antibacterial and biofilm inhibitory activity against the standard and pathogenic *Acinetobacter baumannii* compared to tetracycline. *J. Clust. Sci.*, 33: 1929-1942.

Barabadi, H; Webster, T J; Vahidi, H; Sabori, H; Kamali, K D; Shoushtari, F J; Mahjoub, M A; Rashedi, M; Mostafavi, E; Cruz, D M; Hosseini, O and Saravana, M (2020). Green nanotechnology-based gold nanomaterials for hepatic cancer therapeutics: A systematic review. *Iran. J. Pharm. Res., 19(3)*: 3-17.

Chandana, A; Mallick, S P; Dikshit, P K; Singh, B N and Sahi, A K (2022). Recent developments in bacterial nanocellulose production and its biomedical applications. *J. Polym. Environ., 30*: 4040-4067.

Gan, S; Chen, R S; Mohammad Padzil, F N; Moosavi, S; Tarawneh, M A; Loh, S K and Idris, Z (2023). Potential valorization of oil palm fiber in versatile applications towards sustainability: A review. *Ind. Crops Prod., 199*: 116763.

Ganesh Babu, M M and Gunasekaran, P (2009). Production and structural characterization of crystalline silver nanoparticles from *Bacillus cereus* isolate. *Colloids Surf B: Biointerfaces, 74(1)*: 191-195.

Harrison, T R; Gupta, V K; Alam, P; Perriman, A W; Scarpa, F and Thakur, V K (2023). From trash to treasure: Sourcing high-value, sustainable cellulosic materials from living bioreactor waste streams. *Int. J. Biol. Macromol., 233*: 123511.

Heidari, H; Teimuri, F and Ahmadi, A R (2022). Nanocellulose-based aerogels decorated with Ag, CuO and ZnO nanoparticles: Synthesis, characterization and the antibacterial activity. *Polyhedron, 213*: 115629.

Horue, M; Cacicedo, M L; Fernandez, M A; Rodenak-Kladniew, B; Torres Sánchez, R M and Castro, G R (2020). Antimicrobial activities of bacterial cellulose – Silver montmorillonite nanocomposites for wound healing. *Mater. Sci. Eng. C, 116*: 111152.

Ibraheem, D R; Hussein, N N; Sulaiman, G M; Mohammed, H A; Khan, R A and Al Rugaie, O (2022). Ciprofloxacin-loaded silver nanoparticles as potent nano-antibiotics against resistant pathogenic bacteria. *Nanomater., 12*: 2808.

Jabbari, F and Babaeipour, V (2023). Bacterial cellulose as a potential biopolymer for wound care. A review. *Int. J. Polym. Mater. Polym. Biomater.* DOI: 10.1080/00914037.2023.2167080.

Jain, A S; Pawar, P S; Sarkar, A; Junnuthula, V and Dyawanapelly, S (2021). Bionanofactories for green synthesis of silver nanoparticles: Toward antimicrobial applications. *Int. J. Mol. Sci.*, 22: 11993.

Jutakridsada, P; Suwannaruang, T; Kasemsiri, P; Weerapreeyakul, N; Knijnenburg, J T N; Theerakulpisut, S; Kamwilaisak, K and Chindaprasirt, P (2023). Controllability, antiproliferative activity, Ag^+ release, and flow behavior of silver nanoparticles deposited onto cellulose nanocrystals. *Int. J. Biol. Macromol., 225*: 899-910.

Li, Z; Wang, L; Chen, S; Feng, C; Chen, S; Yin, N; Yang, J; Wang, H and Xu, Y (2015). Facilely green synthesis of silver nanoparticles into bacterial cellulose. *Cellulose, 22(1)*: 373-383.

Lim, H J; Cheng, W K; Tan, K W and Yu, L J (2022). Oil palm-based nanocellulose for a sustainable future: Where are we now? *J. Environ. Chem. Eng., 10(2)*: 107271.

Lin, W C; Lien, C C; Yeh, H J; Yu, C M and Hsu, S H (2013). Bacterial cellulose and bacterial cellulose-chitosan membranes for wound dressing applications. *Carbohydr. Polym., 94(1)*: 603-611.

Liu, Y; Lu, T; Sun, Z; Chua, D H C and Pan, L (2015). Ultra-thin carbon nanofiber networks derived from bacterial cellulose for capacitive deionization. *J. Mater. Chem. A, 3(16)*: 8693-8700.

Manosalva, N; Tortella, G; Cristina Diez, M; Schalchli, H; Seabra, A B; Durán, N and Rubilar, O (2019). Green synthesis of silver nanoparticles: Effect of synthesis reaction parameters on antimicrobial activity. *World J. Microbiol. Biotechnol., 35(6)*: 1-9.

Mohamad, S; Abdullah, L C; Jamari, S S; Osman Al Edrus, S S; Aung M M and Mohamad, S F S (2022). Production and characterization of bacterial cellulose nanofiber by *Acetobacter xylinum* 0416 using only oil palm frond juice as fermentation medium. *J. Nat. Fibers, 19(17)*: 16005–16016.

More, P R; Pandit, S; Filippis, A D; Franci, G; Mijakovic, I and Galdiero, M (2023). Silver nanoparticles: Bactericidal and mechanistic approach against drug resistant pathogens. *Microorganisms, 11*: 369.

Norrrahim, M N F; Farid, M A A; Lawal, A A; Tengku Yasim-Anuar, T A; Samsudin, M H and Zulkifli, A A (2022). Emerging technologies for value-added use of oil palm biomass. *Environ. Sci.: Advances, 1(3)*: 259-275.

Pal, S; Nisi, R; Stoppa, M and Licciulli, A (2017). Silver-functionalized bacterial cellulose as antibacterial membrane for wound-healing applications. *ACS Omega, 2(7)*: 3632-3639.

Pang, M; Huang, Y; Meng, F; Zhuang, Y; Liu, H and Du, M (2020). Application of bacterial cellulose in skin and bone tissue engineering. *Eur. Polym. J., 122*: 109365.

Parveez, G K A; Rasid, O A; Ahmad, M N; Taib, H M; Bakri, M A M; Hafid, S R A; Ismail, T N M T; Loh, S K; Abdullah, M O; Zakaria, K and Idris, Z (2023). Oil palm economic performance in Malaysia and R&D progress in 2022. *J. Oil Palm Res., 35(2)*: 193-216.

Qiu, Y; Qiu, L; Cui, J and Wei, Q (2016). Bacterial cellulose and bacterial cellulose-vaccarin membranes for wound healing. *Mater. Sci. Eng. C, 59*: 303-309.

Rashidi, N A; Chai, Y H and Yusup, S (2022). Biomass energy in Malaysia: Current scenario, policies, and implementation challenges. *BioEnergy Res., 15*: 1371-1386.

Sabarees, G; Velmurugan, V; Tamilarasi, G P; Alagarsamy, V and Raja Solomon, V (2022). Recent advances in silver nanoparticles containing nanofibers for chronic wound management. *Polymers, 14*: 3994.

Said Azmi, S N N; Samsu, Z A; Mohd Asnawi, A S F; Ariffin, H and Syed Abdullah, S S (2023). The production and characterization of bacterial cellulose pellicles obtained from oil palm frond juice and their conversion to nanofibrillated cellulose. *Carbohydr. Polym. Technol. Appl., 5*: 100327.

Saravanan, M; Barabadi, H; Vahidi, H; Webster, T J; Medina-Cruz, D; Mostafavi, E; Vernet-Crua, A; Cholula-Diaz, J L and Periakaruppan, P (2021). Emerging theranostic silver and gold nanobiomaterials for breast cancer: Present status and future prospects. *Handbook on Nanobiomaterials for Therapeutics and Diagnostic Applications* (Anand, K; Saravanan, M; Chandrasekaran, B; Kanchi, S; Panchu, S J and Chen, Q S eds.). Elsevier. p. 439-456.

Shaaban, M T; Zayed, M and Salama, H S (2023). Antibacterial potential of bacterial cellulose impregnated with green synthesized silver nanoparticle against *S. aureus* and *P. aeruginosa*. *Curr. Microbiol., 80(2)*: 1-9.

Shidlovskiy, I P; Shumilova, A A; Shishatskaya, E I and Volova, T G (2018). Properties of bacterial cellulose composites with silver nanoparticles. *Biophys., 63(4)*: 519-525.

Talank, N; Morad, H; Barabadi, H; Mojab, F; Amidi, S; Kobarfard, F; Mahjoub, M A; Jounaki, K; Mohammadi, N; Salehi, G; Ashrafizadeh, M and Mostafavi, E

(2022). Bioengineering of green-synthesized silver nanoparticles: *In vitro* physicochemical, antibacterial, biofilm inhibitory, anticoagulant, and antioxidant performance. *Talanta*, *243*: 123374.

Volova, T G; Shumilova, A A; Shidlovskiy, I P; Nikolaeva, E D; Sukovatiy, A G; Vasiliev, A D and Shishatskaya, E I (2018). Antibacterial properties of films of cellulose composites with silver nanoparticles and antibiotics. *Polym. Test., 65*: 54-68.

Wu, J; Zheng, Y; Song, W; Luan, J; Wen, X; Wu, Z; Chen, Z; Wang, Q and Guo, S (2014). *In situ* synthesis of silver-nanoparticles/bacterial cellulose composites for slow-released antimicrobial wound dressing. *Carbohydr. Polym., 102(1)*: 762-771.

Yang, G; Xie, J; Hong, F; Cao, Z and Yang, X (2012). Antimicrobial activity of silver nanoparticle impregnated bacterial cellulose membrane: Effect of fermentation carbon sources of bacterial cellulose. *Carbohydr. Polym., 87(1)*: 839-845.

Zakaria, M R; Ahmad Farid, M A; Andou, Y; Ramli, I and Hassan M A (2023). Production of biochar and activated carbon from oil palm biomass: Current status, prospects, and challenges. *Ind. Crops Prod., 199*: 116767.

Zeng, M; Laromaine, A and Roig, A (2014). Bacterial cellulose films: Influence of bacterial strain and drying route on film properties. *Cellulose, 21(6)*: 4455-4469.